First-principles study of structural and electronic properties of ultrathin silicon nanosheets

Tetsuya Morishita,[1,2,*] Salvy P. Russo,[1] Ian K. Snook,[1] Michelle J. S. Spencer,[1] Kengo Nishio,[2] and Masuhiro Mikami[2]
[1]*Applied Physics, School of Applied Sciences, RMIT University, GPO Box 2476, Melbourne, Victoria 3001, Australia*
[2]*Research Institute for Computational Sciences (RICS), National Institute of Advanced Industrial Science and Technology (AIST), 1-1-1 Umezono, Tsukuba, Ibaraki 305-8568, Japan*

(Received 16 November 2009; revised manuscript received 28 May 2010; published 20 July 2010)

Silicon (Si) is currently the basis of most of our nanodevice technology and ultrathin materials based on Si would have the great advantage of easy integration into existing circuitry. Recently, it has been demonstrated using molecular-dynamics calculations that two-dimensional ultrathin layered Si can be formed by cooling fluid Si confined in a slit pore [T. Morishita *et al.*, Phys. Rev. B **77**, 081401(R) (2008)]. Here we investigate, using *ab initio* density-functional theory, the structural and electronic properties of ultrathin double layer Si with and without hydrogenation or substitutional doping. We show that such materials have very desirable electronic properties, being able to be changed from metallic to semiconducting. They may also act as *p*-type or *n*-type semiconductors upon partial hydrogenation or substitutional doping of phosphorus. We suggest that these materials may be of great importance to production of nanoelectronic devices and sensors.

DOI: 10.1103/PhysRevB.82.045419 PACS number(s): 73.22.−f, 62.23.Kn, 61.46.Hk, 31.15.es

I. INTRODUCTION

Nanostructured materials have and continue to attract intense interest because of their often unique and potentially useful properties.[1–3] An enormous amount of research work has been carried out on zero-dimensional (0D) and one-dimensional (1D) nanostructures[4–12] and such systems are now being used in practical applications.[13–15] However, less work has been reported on two-dimensional (2D) nanosystems,[16] the exceptions being work on graphene[17,18] and more recently planar boron nitride.[19–22] Graphene has proved to be fascinating both from a basic scientific point of view and with respect to potential applications in many areas such as sensors and transistors.[23,24] In particular, graphene holds great promise as the basis of the next generation of nanoscale electronic devices. However, graphene does suffer several problems for large scale, practical applications in this area, e.g., the controlled fabrication of structures and its zero-band-gap semimetallic character.[18] Thus, silicon (Si) may prove easier to implement in device nanofabrication.

Much of modern microelectronics is based on exploiting the properties of Si and an enormous amount of knowledge is available to assist in designing and fabricating Si-based devices. Thus, it would seem to be extremely worthwhile to investigate the possibility of producing nanodevices based on Si. 0D Si nanostructures, i.e., quantum dots, and 1D Si nanostructures, i.e., nanowires (NWs), are being actively investigated and potential practical devices such as field-effect transistors (FETs) and sensors may be fabricated from them.[13–15] However, much less is known about 2D Si-based nanostructures[25–27] which may be useful to form the basis of nanoelectronic devices. In fact, 2D structures can easily accommodate current silicon-on-insulator (SOI) technology for FETs, in which very thin channel thickness is highly desirable.[25]

Very recently it has been demonstrated experimentally and theoretically that it is possible to fabricate 2D Si-based nanomaterials.[28–30] In particular, our previous molecular-dynamics (MD) calculations have demonstrated that 2D structures consisting of a single layer (SL) and double layers (DLs) of Si may be formed from liquid Si confined in pores.[30] This is analogous to the way Si NWs may be fabricated in practice.[31] Unfortunately, free-standing graphenelike planar SL-Si has been shown theoretically by density-functional theory (DFT) to be unstable.[32] However, so far the properties of DL-Si have not been investigated.

Thus, in this study we use *ab initio* DFT at the generalized-gradient approximation (GGA) level to investigate the geometry and electronic structures of free-standing DL-Si nanosheets in order to see if such systems have promising electronic properties. This is done for pure Si systems and for systems with varying degrees of hydrogenation or substitution by other elements.

The paper is organized as follows. In Sec. II, our models and calculation method are briefly given. Section III shows the geometry and electronic structures of unpassivated, partially passivated, and fully passivated DL-Si, and Sec. IV summarizes our findings.

II. MODELS AND COMPUTATIONAL METHOD

We consider in this paper DL-Si systems with and without dangling bonds (DBs). Figure 1(a) shows DL-Si that consists of two corrugated infinite hexagonal layers (note that only atoms in the supercell are shown in Fig. 1). Atoms in the upper layer are superimposed on those in the lower layer, which can be viewed as a part of the hexagonal diamond structure if the bond lengths in *a* and *b* directions have the same length (Fig. 1). It has been demonstrated[30] that this type of DL-Si can be formed by cooling liquid Si confined in a slit nanopore in MD calculations using the Tersoff model.[33] In this work, we use the final structure from the Tersoff MD calculation as our initial structures for geometry optimization.

The outermost atoms in the *z* direction are three-coordinated (undercoordinated), thus there exist DBs on these surface Si atoms. To model the DL-Si systems without the DBs, we saturated the DBs by (1) hydrogenation [Fig.

 ©2010 The American Physical Society

1(b): DL-Si:H] or (2) substitutional doping of phosphorus (P) for the surface Si atoms [Fig. 1(c): DL-SiP]. We also modeled DL-Si with partially saturated DBs using these two methods.

We used a rectangular-parallelepiped supercell with periodic boundary conditions for all the DL-Si systems we focus on in this paper: the supercell contains 64 Si atoms for DL-Si, 64 Si and 32 H atoms for DL-Si:H, and 32 Si and 32 P atoms for DL-SiP (see Fig. 1). The vacuum space of approximately 12 Å is accommodated along the z direction [Fig. 1(d)]. Electronic structures were calculated after geometry relaxation throughout which no geometrical constraint was imposed in all the systems. We also used the primitive unit cell [as shown in Fig. 1(b)] to obtain the band structure for the three DL-Si systems.

All the calculations were performed in the framework of DFT with the projector-augmented wave method[34] and the generalized-gradient approximation for the exchange and correlation energy functional[35] using the Vienna *ab initio* simulation package.[36] The electronic wave functions were expanded in a plane-wave basis with an energy cutoff of 250 eV for DL-Si, 300 eV for DL-Si:H, and 270 eV for DL-SiP. The Brillouin zone was sampled by $(8\times8\times1)$ and $(32\times32\times1)$ mesh points for the rectangular-parallelepiped supercell and the primitive unit cell, respectively, which are found to be sufficient in this case by preliminary testing. Atomic positions as well as the supercell volume were relaxed with the maximum force tolerance of 0.01 eV/Å and the maximum stress tolerance of 0.5 kbar, unless otherwise specified. For partially hydrogenated DL-Si, we used the same cell as that for DL-Si:H while for partially doped DL-Si, the supercell was relaxed for each system having a different doping ratio. This is because the maximum stress in the partially hydrogenated DL-Si is at most approximately 2 kbars while that in the partially doped DL-Si exceeds 35 kbar.

III. RESULTS AND DISCUSSION

A. Atomic configuration

Table I summarizes the bond lengths and bond angles in the three DL-Si systems [a, b, θ, and ϕ; see Fig. 1(a)]. In DL-Si [Fig. 1(a)], the length of the Si-Si in-plane bond (a) is 2.32 Å while that of the interplane bond (b) is 2.47 Å. The latter is slightly longer than the Si-Si bond in bulk-crystalline Si (c-Si) (2.352 Å), which is likely due to the existence of the three-coordinated Si atoms in DL-Si (see also below). The angle between the in-plane bonds (θ) is 112.2°, being slightly larger than the regular tetrahedral angle of 109.5°. This indicates that each hexagonal layer has a more planar structure than its counterpart in bulk c-Si. The angle between the in-plane and interplane bonds (ϕ) is, in fact, 106.6°, being smaller than 109.5°. It is likely that DL-Si exhibits reconstruction due to the DBs (the surface geometry is the same as that of an ideal bulk (111) plane). In the geometry optimization from an ideal hexagonal configuration, however, we found this ideal surface structure is at least locally stable (our preliminary *ab initio* MD calculation also supports this). The stability of this structure at high temperatures deserves future investigation and will be reported elsewhere.

TABLE I. Bond length and bond angle in the DL-Si systems (see Fig. 1).

	a (Å)	b (Å)	θ (deg)	ϕ (deg)
DL-Si	2.32	2.47	112.2	106.6
DL-Si:H	2.36	2.38	109.2–109.8	109.2–109.8
DL-SiP	2.28	2.38	101.5	116.6

The bond length in a and b directions in DL-Si:H are 2.36 Å and 2.38 Å, respectively. By saturating the DBs on the three-coordinated Si atoms, the interplane bond length becomes much closer to the bulk Si-Si bond length (2.352 Å) than in DL-Si. The Si-H bond length is 1.51 Å, which is close to the Si-H bond length in a SiH_4 molecule (1.47 Å). The bond angles, θ and ϕ, are in the range of 109.2°–109.8° and are almost equal to the regular tetrahedral angle.

The interplane (Si-Si) bond length in DL-SiP is the same as that in DL-Si:H (b=2.38 Å) while the Si-P bond length is 2.28 Å, being shorter than any Si-Si bonds in the DL-Si systems. We are not aware of a bulk crystalline forms of SiP but a recent DFT study for a possible crystalline form of Si_3P_4 reports that the Si-P bond length is about 2.25 Å.[37] The Si-P-Si bond angle is 101.5° while the Si-Si-P bond angle is 116.6°, indicating that the hexagonal layers in DL-SiP are more corrugated than those in DL-Si and DL-Si:H. This corrugation is consistent with the fact that P atoms are three-coordinated by covalent bonds composed of p electrons only in its crystalline forms, resulting in the bond angle of 96°–102° (Ref. 38) (we again discuss this corrugated structure later on). It should be remarked in passing that the DB-saturated DL-Si has been found to be stable at room temperature in our preliminary *ab initio* MD runs.

B. Electronic structure

1. Band structure

The band structure for DL-Si, DL-Si:H, and DL-SiP is shown in Fig. 2. The band energy is measured from the highest occupied level at T=0 K (zero temperature). Also shown is the band structure for a bulklike hexagonal diamond Si in which no DB is formed; the bulklike Si is modeled by removing the vacancy space in the supercell for DL-Si and by subsequent geometry optimization (the in-plane Si-Si bond length is 2.36 Å while the interplane Si-Si bond length is 2.38 Å). We clearly see that DL-Si is metallic whereas DL-Si:H and DL-SiP have an indirect band gap. Comparing the band structure for DL-Si and that for the bulklike hexagonal diamond Si, the bands near the Fermi energy (E_F=0 eV) in DL-Si can be identified as those associated with the surface Si atoms having DBs (the DB bands). The contour plots of the electron-localization function (ELF),[39,40] which is the measure of electron localization and takes higher values for more highly localized electrons (ranging from 0 to 1), at the bottom of Fig. 2 indicate that electrons in the vicinity of

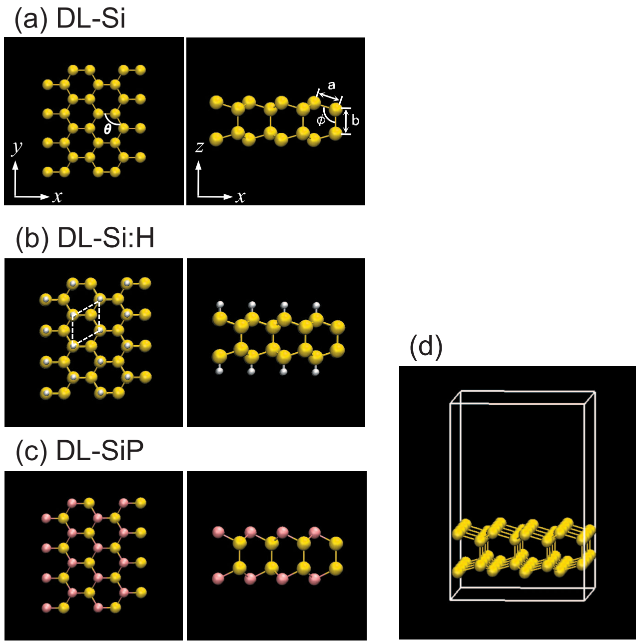

FIG. 1. (Color) Atomic configurations for (a) DL-Si, (b) DL-Si:H, and (c) DL-SiP in the rectangular-parallelepiped supercells (no image atoms due to the periodic boundary conditions are shown). Yellow, white, and pink balls denote Si, H, and P atoms, respectively. The supercell geometry is illustrated in (d) while the primitive unit cell is indicated by dashed lines in (b).

atoms with DBs (indicated by arrows) are less localized than those forming covalent bonds (regions represented in red between bonding atoms). This is consistent with the highly dispersive DB band which, interestingly, appears more dispersive than its counterpart of an ideal bulk Si (111) surface.[41]

The DBs can be saturated by supplying extra electrons. In DL-Si:H, hydrogenation clearly removes the DB bands near the E_F, which then contribute to the formation of σ bonds between Si and H atoms. Substitutional doping of P also results in the saturation of the DBs because P has one extra valence electron compared to Si. Interestingly, in the energy range of $-5-0$ eV, the band profile of DL-SiP is very similar to that of DL-Si. This is consistent with the similar ELF contour plot in DL-Si and DL-SiP. DL-Si:H exhibits a rather different band profile, which may be due to the strongly localized electrons induced by the formation of Si-H bonds (see the contour plot of ELF).

It is worth noting that the band gap of the bulklike hexagonal diamond Si (approximately 0.5 eV) (Ref. 42) is smaller than that of the cubic diamond c-Si (approximately 0.7 eV),[42] although all Si atoms are tetrahedrally four-coordinated by covalent bonds in both systems. The reason for this difference in the electronic structure is yet to be clarified but this difference should be related to the greater stability of the cubic diamond structure than the hexagonal diamond structure of Si in practice.[43,44]

2. Density of states

Figures 3–5 show the electronic density of states (DOS) for DL-Si, DL-Si:H, and DL-SiP, respectively. As shown in

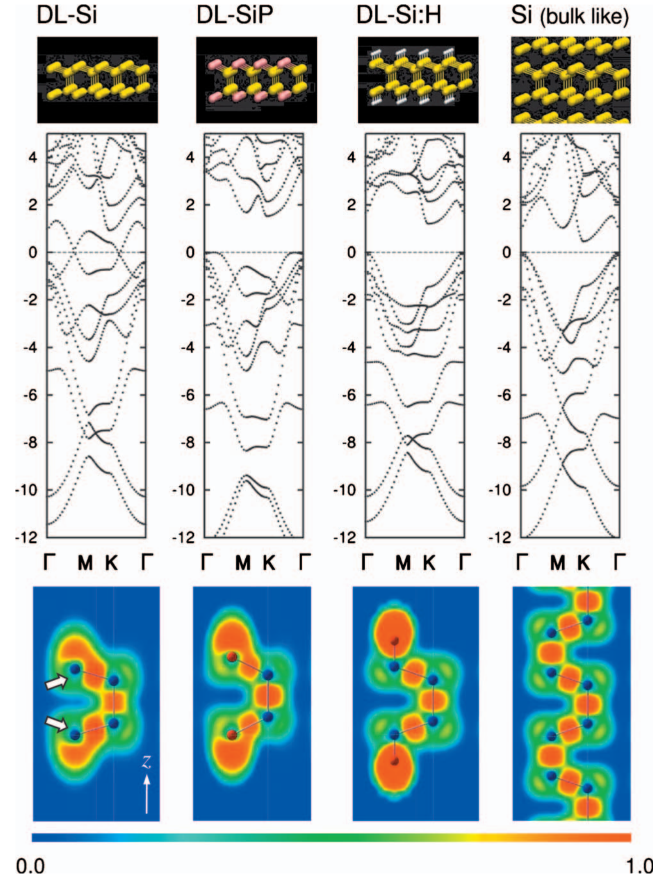

FIG. 2. (Color) Band structure for the three DL-Si systems and the bulklike hexagonal diamond Si (see text). The band energy is measured from the highest occupied level at $T=0$ K. The contour plots of the ELF for each system are shown at the bottom. Note that the ELF shows the degree of localization of electrons but not electron density itself. Arrows in the ELF plot for DL-Si indicate surface Si atoms having DBs.

the band structure (Fig. 2), the total DOS for DL-Si [Fig. 3(a)] exhibits no energy gap at E_F (0 eV). The partial DOS for the four-coordinated and three-coordinated Si atoms are given in Figs. 3(b) and 3(c), respectively. We clearly see that the bands near the E_F mainly come from p_z electrons of the three-coordinated atoms (surface Si atoms). This indicates that the DBs are mainly composed of p_z electrons. In the four-coordinated Si atoms [Fig. 3(b)], on the other hand, an appreciable contribution of p_z electrons to the valence bands below -2 eV, which should be σ bands, is found.

The total DOS for DL-Si:H shows a clear band gap of about 1.2 eV. The p_z bands of the hydrogenated Si [Fig. 4(c)] almost overlap the s bands of the H atoms [Fig. 4(d)], indicating the formation of strong Si-H bonds. As already mentioned, the electrons associated with the Si-H bonds are highly localized around the H atoms (Fig. 2).

Figure 5(a) shows that DL-SiP has a slightly wider band gap (around 1.5 eV) than that of DL-Si:H. In the crystalline forms of P (A17 and A7 forms),[38] P atoms are bonded to each other by covalent bonds composed of p electrons only; each P atom is thus three-coordinated and the bond angle is $96°-102°$ in A17 and A7 crystalline forms. These character-

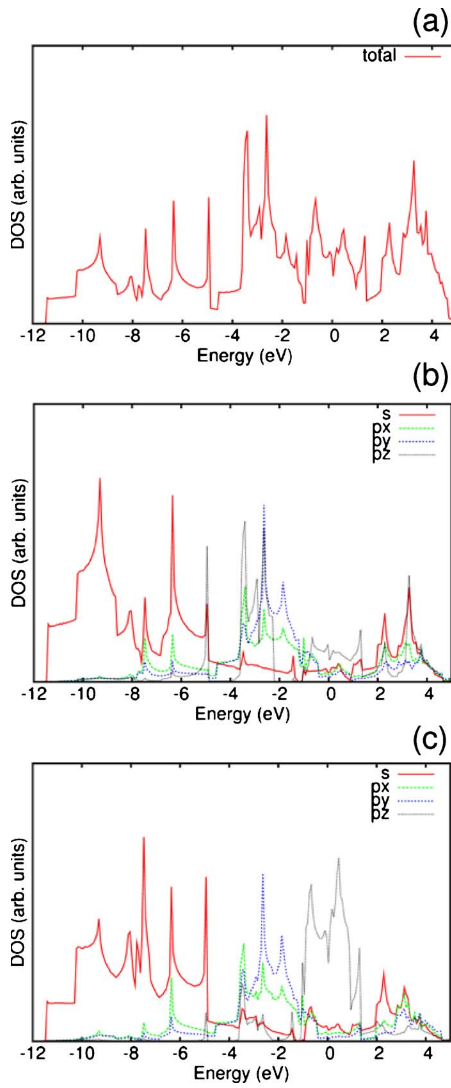

FIG. 3. (Color online) DOS for DL-Si: (a) total DOS, (b) partial DOS for the four-coordinated Si atoms, and (c) partial DOS for the three-coordinated Si atoms. The energy is measured from the highest occupied level at $T=0$ K.

istics can also be recognized in DL-SiP from the partial DOS for P [Fig. 5(c)]. The bands below approximately −9 eV in the partial DOS for P mainly come from *s* electrons and their contribution to the valence bands between −8 and 0 eV is less than the Si *s* electron contribution [Fig. 5(b)] within the same regions. In other words, sp^3 hybridization remains in Si while *p* electrons mainly dominate the valence bands above −8 eV in P. This finding is consistent with the relatively corrugated layer structure in DL-SiP, in which the Si-P-Si bond angle is closer to 90° than the corresponding angle in DL-Si (see Sec. III A) because of the dominant contribution of *p* electrons to the Si-P bond. We note that the overall shape of the p_z bands closely resembles that in DL-Si. This reflects the strong similarity of the band structure in DL-SiP and DL-Si as discussed in Sec. III B 1.

3. Partial DB saturation

In this section we discuss the effect of partial DB saturation in DL-Si. Figure 6 shows the dependence of the DOS

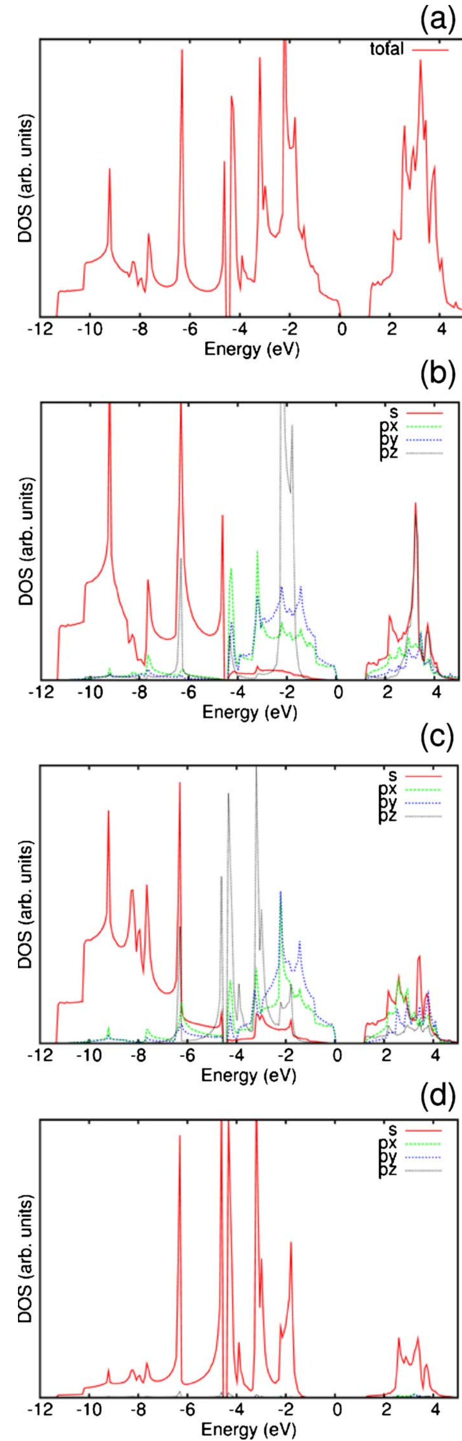

FIG. 4. (Color online) DOS for DL-Si:H: (a) total DOS, (b) partial DOS for the four-coordinated Si atoms, (c) partial DOS for the hydrogenated Si atoms, and (d) partial DOS for H. The energy is measured from the highest occupied level at $T=0$ K.

for DL-Si on the hydrogenation ratio. It is clearly seen that as the hydrogenation ratio increases, the band gap opens up (as well as a pseudogap at 0.5–1 eV).[45] Over approximately 50% hydrogenation, localized gap states emerge and they become more localized as the hydrogenation ratio increases. Over approximately 80% hydrogenation, the gap states are highly localized and they may be regarded as acceptor states

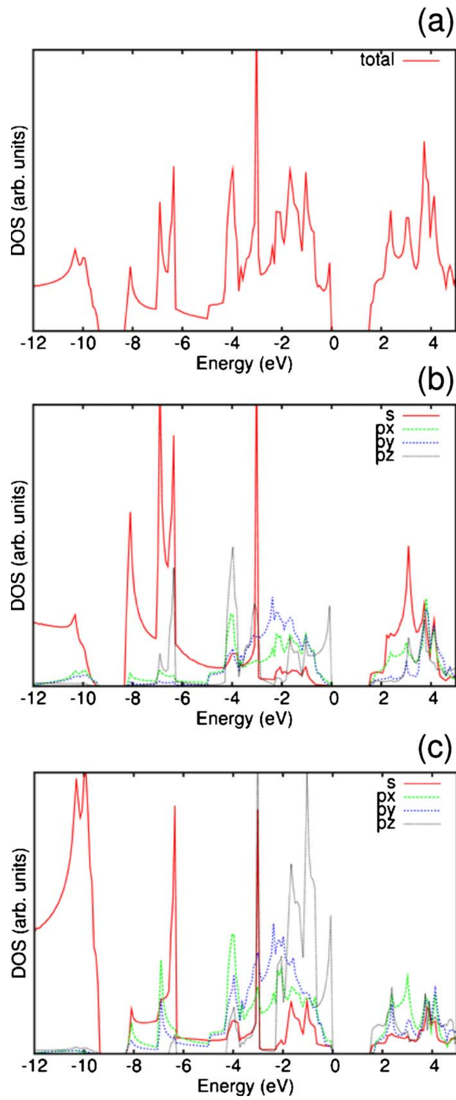

FIG. 5. (Color online) DOS for DL-SiP: (a) total DOS, (b) partial DOS for the Si atoms, and (c) partial DOS for the P atoms. The energy is measured from the highest occupied level at $T=0$ K.

in a p-type semiconductor. That is, partially hydrogenated DL-Si can be a p-type semiconductor.

Similar to the partial hydrogenation in DL-Si, partial substitution of P is also able to produce a p-type semiconductor. In Fig. 7, we find that localized gap states are formed with substitutional doping of P in DL-Si at levels of over 50%. These localized states are just above the top of the valence bands, so they may act as acceptor states (p-type semiconductor). Surprisingly, the gap states disappear with substitutional doping at levels of over 93%. This may indicate that the DBs on unreplaced surface Si atoms are so highly localized that no electrons in the DBs can participate in electronic conduction.

Doping P atoms into bulk c-Si normally generates an n-type semiconductor, in contrast to the doping in the DL-Si systems. In the c-Si case, four of the five valence electrons of a P atom participate in forming tetrahedral covalent bonds, thus an extra one electron induces donor states resulting in n-type semiconductor. In contrast, imperfect substitution of P

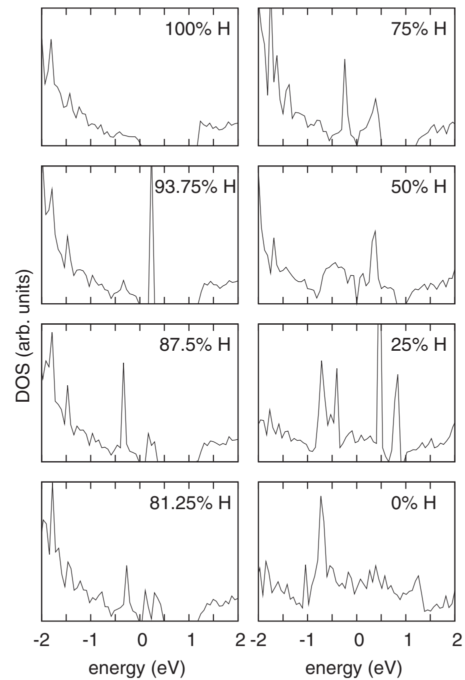

FIG. 6. DOS for partially hydrogenated DL-Si as a function of hydrogenation ratio. The energy is measured from the highest occupied level at $T=0$ K.

in DL-Si causes a deficiency of electrons compared to the perfect substitution (DL-SiP). Therefore, an unreplaced Si atom in an imperfect DL-SiP acts like a boron (B) or aluminum (Al) impurity in c-Si, which in this case results in a p-type semiconductor.

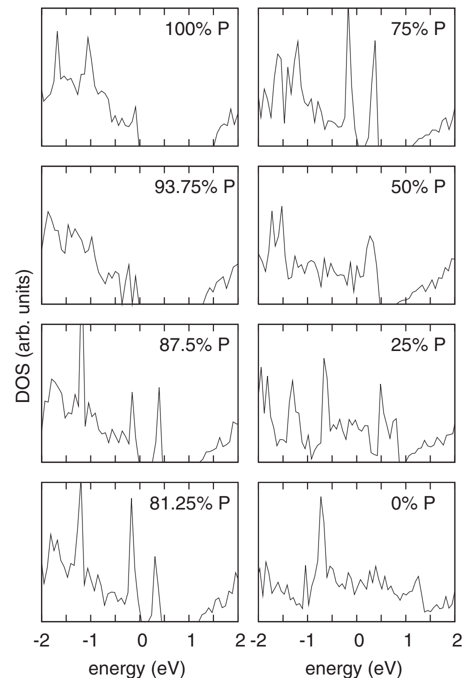

FIG. 7. DOS for partially doped DL-Si as a function of P-doping ratio. The energy is measured from the highest occupied level at $T=0$ K.

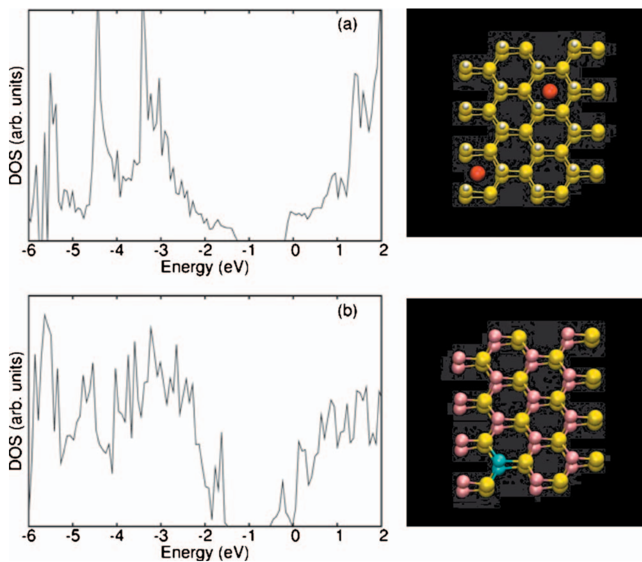

FIG. 8. (Color) DOS for (a) Na-doped DL-Si:H and (b) S-doped DL-SiP (see text). The energy is measured from the highest occupied level at $T=0$ K. The corresponding atomic configurations are displayed in the right panels in which Na and S atoms are denoted by red and blue balls, respectively.

By extending this concept, we can also produce *n*-type DL-Si semiconductors. To this end, we consider interstitial doping of sodium (Na) atoms in DL-Si:H and partial replacement of P atoms with sulfur (S) atoms in DL-SiP. In both systems, Na or S atoms can work as a donor of electrons resulting in an *n*-type semiconductor. Figure 8 shows the DOS for DL-Si:H with two interstitial Na atoms ($Si_{64}H_{32}Na_2$) and that for DL-SiP with the substitution of two P atoms for two S atoms ($Si_{32}P_{30}S_2$). It is clearly shown that both systems exhibit donor states near the conduction band minimum (0 eV). Note that interstitial doping of Na has also been attempted in a hydrogenated polyicosahedral Si NW and similar modification in the electronic structure was observed.[12]

In hydrogenated Si NWs, doping of P results in an *n*-type semiconductor as in c-Si.[8–11] This indicates that substitutional doping of P in DL-Si:H is expected to produce an *n*-type semiconductor as well (and doping by B or Al should produce a *p*-type semiconductor). It is thus likely that a variety of methods can apply to the DL-Si systems to obtain a *p*- or *n*-type semiconductor, which will be of importance in building an ultrathin FET based on the DL-Si systems.

IV. CONCLUSIONS

We have clarified the geometry and electronic structures of DL-Si systems using plane-wave-based DFT-GGA calculations. We have shown that the electronic structure strongly depends on the amount of the DBs on the surface Si atoms in the DL-Si systems. The band structure and DOS for DL-Si, in which all surface Si atoms are three-coordinated (one DB for one Si atom), clearly show that DL-Si is metallic. The DL-Si systems without any DBs, in contrast, exhibit a semiconducting nature. We have adopted two methods to eliminate the DBs; hydrogenation and substitutional doping of P. Both methods produce semiconductors with an indirect band gap of 1.2 eV (DL-Si:H) or 1.5 eV (DL-SiP). We found from the partial DOS that p_z electrons play a crucial role in characterizing the electronic structure of the DL-Si systems.

We also examined the effect of partially saturated DBs by partial hydrogenation and partial doping of P. We have shown that unsaturated DBs can work as acceptors giving rise to acceptor states just above the valence band maximum (*p*-type semiconductor). Interstitial doping of Na and substitution of S are, on the other hand, found to generate *n*-type semiconductors in DL-Si:H and DL-SiP, respectively. It has been demonstrated that either a *p*- or *n*-type semiconductor can be produced based on the DL-Si systems. The DL-Si systems are highly compatible with SOI technology that has been introduced to reduce parasitic device capacitance in conventional Si-built FET devices. We therefore consider that the DL-Si systems are a possible candidate material for future nanoscale electronic devices such as an ultrathin FET.

ACKNOWLEDGMENTS

This work is supported by the National Computational Infrastructure (NCI) National Facility, Australia, and New Energy and Industrial Technology Development Organization (NEDO), Japan. The computations were in part carried out at the Research Center for Computational Science, National Institute of Natural Sciences, Japan.

*t-morishita@aist.go.jp; http://staff.aist.go.jp/t-morishita/

[1] D. Appell, Nature (London) **419**, 553 (2002).
[2] A. S. Barnard, J. Mater. Chem. **16**, 813 (2006).
[3] *Nanoscience and Nanotechnology*, The royal Society: http://www.nanotec.org.uk
[4] R. Ferrando, J. Jellinek, and R. L. Johnston, Chem. Rev. **108**, 845 (2008).
[5] K. Koga and K. Sugawara, Surf. Sci. **529**, 23 (2003).
[6] A. S. Barnard, S. P. Russo, and I. K. Snook, Philos. Mag. B **83**, 2301 (2003); **83**, 2311 (2003).
[7] K. Nishio, T. Morishita, W. Shinoda, and M. Mikami, Phys. Rev. B **72**, 245321 (2005); J. Chem. Phys. **125**, 074712 (2006).
[8] A. K. Singh, V. Kumar, R. Note, and Y. Kawazoe, Nano Lett. **6**, 920 (2006).
[9] M. V. Fernández-Serra, C. Adessi, and X. Blase, Phys. Rev. Lett. **96**, 166805 (2006).
[10] E. Durgun, N. Akman, C. Ataca, and S. Ciraci, Phys. Rev. B **76**, 245323 (2007).
[11] C. R. Leao, A. Fazzio, and A. J. R. da Silva, Nano Lett. **8**, 1866 (2008).
[12] K. Nishio, T. Ozaki, T. Morishita, W. Shinoda, and M. Mikami, Phys. Rev. B **77**, 075431 (2008).

[13] Y. Cui and C. M. Lieber, Science **291**, 851 (2001).
[14] B. K. Teo and X. H. Sun, Chem. Rev. **107**, 1454 (2007).
[15] V. Kumar, *Nanosilicon* (Elsevier, Amsterdam, 2008).
[16] S. Lebègue and O. Eriksson, Phys. Rev. B **79**, 115409 (2009).
[17] A. K. Geim and K. S. Novoselov, Nature Mater. **6**, 183 (2007).
[18] A. Cresti, N. Nemec, B. Biel, G. Niebler, F. Triozon, G. Cuniberti, and S. Roche, Nano Res. **1**, 361 (2008).
[19] A. Nagashima, N. Tejima, Y. Gamou, T. Kawai, and C. Oshima, Phys. Rev. Lett. **75**, 3918 (1995).
[20] C. Zhi, Y. Bando, C. Tang, D. Golberg, R. Xie, and T. Sekiguchi, Appl. Phys. Lett. **87**, 063107 (2005).
[21] F. Zheng, G. Zhou, Z. Liu, J. Wu, W. Duan, B. L. Gu, and S. B. Zhang, Phys. Rev. B **78**, 205415 (2008).
[22] M. Topsakal, E. Aktürk, and S. Ciraci, Phys. Rev. B **79**, 115442 (2009).
[23] I. Meric, M. Y. Han, A. F. Young, B. Ozyilmaz, P. Kim, and K. L. Shepard, Nat. Nanotechnol. **3**, 654 (2008).
[24] R. M. Westervelt, Science **320**, 324 (2008).
[25] T. Miyazaki and T. Kanayama, Appl. Phys. Lett. **91**, 082107 (2007); Jpn. J. Appl. Phys., Part 2 **46**, L28 (2007).
[26] T. He, H. Zhang, Z. Wang, X. Zhang, Z. Xi, X. Liu, M. Zhao, Y. Xia, and L. Mei, Physica E **41**, 1795 (2009).
[27] H. Nakano, T. Mitsuoka, M. Harada, K. Horibuchi, H. Nozaki, N. Takahashi, T. Nonaka, Y. Seno, and H. Nakamura, Angew. Chem. **118**, 6451 (2006).
[28] H. Okamoto, Y. Kumai, Y. Sugiyama, T. Mitsuoka, K. Nakanishi, T. Ohta, H. Nozaki, S. Yamaguchi, S. Shirai, and H. Nakano, J. Am. Chem. Soc. **132**, 2710 (2010).
[29] Y. Sugiyama, H. Okamoto, T. Mitsuoka, T. Morikawa, K. Nakanishi, T. Ohta, and H. Nakano, J. Am. Chem. Soc. **132**, 5946 (2010).
[30] T. Morishita, K. Nishio, and M. Mikami, Phys. Rev. B **77**, 081401(R) (2008).
[31] D. Buttard, T. David, P. Gentile, M. Den Hertog, T. Baron, P. Ferret, and J. L. Rouviére, Phys. Status Solidi A **205**, 1606 (2008); D. Buttard, T. David, P. Gentile, F. Dhalluin, and T. Baron, Phys. Status Solidi (RRL) **3**, 19 (2009).
[32] S. Cahangirov, M. Topsakal, E. Aktürk, H. Sahin, and S. Ciraci, Phys. Rev. Lett. **102**, 236804 (2009).
[33] J. Tersoff, Phys. Rev. B **39**, 5566 (1989).
[34] P. E. Blöchl, Phys. Rev. B **50**, 17953 (1994).
[35] J. P. Perdew, K. Burke, and M. Ernzerhof, Phys. Rev. Lett. **77**, 3865 (1996).
[36] G. Kresse and J. Furthmüller, Comput. Mater. Sci. **6**, 15 (1996); Phys. Rev. B **54**, 11169 (1996).
[37] M. Huang, Y. P. Feng, A. T. L. Lim, and J. C. Zheng, Phys. Rev. B **69**, 054112 (2004).
[38] Y. Maruyama, S. Suzuki, K. Kobayashi, and S. Tanuma, Physica B & C **105**, 99 (1981); Y. Takao and A. Morita, *ibid.* **105**, 93 (1981).
[39] A. D. Becke and K. E. Edgecombe, J. Chem. Phys. **92**, 5397 (1990).
[40] B. Silvi and A. Savin, Nature (London) **371**, 683 (1994).
[41] M. Schlüter, J. R. Chelikowsky, S. G. Louie, and M. L. Cohen, Phys. Rev. B **12**, 4200 (1975).
[42] This energy value is from our DFT calculations, in which the band gap is generally underestimated.
[43] M. R. Salehpour and S. Satpathy, Phys. Rev. B **41**, 3048 (1990).
[44] A. S. Barnard, S. P. Russo, and I. K. Snook, Philos. Mag. B **82**, 1767 (2002).
[45] Note that similar behavior has been found in hydrogenated carbon diamond NWs: A. S. Barnard, S. P. Russo, and I. K. Snook, Phys. Rev. B **68**, 235407 (2003); A. S. Barnard, Ph.D. thesis, RMIT University, 2003.